Local Stereoscopic Field Singularity Models for FDTD Analysis of Guided Wave Problems

Malgorzata Celuch - Marcysiak

Institute of Radioelectronics, Warsaw University of Technology,
ul.Nowowiejska 15/19, Warsaw 03-938, Poland, E-mail: m.celuch@ire.pw.edu.pl

ABSTRACT – **New local FDTD field singularity models have been proposed. In extension to previous local models, not only radial field variation but also the geometry of field lines and curvature of Ampere / Faraday integration surfaces are taken into account. The method is shown to provide the same order of accuracy as previously published specialised higher-order algorithms. Yet contrary to those methods the gain in accuracy is achieved practically without any increase of the computing time of FDTD simulations.**

I. INTRODUCTION

The necessity to introduce special models for metal strips and slots into the space-discrete methods like FDTD or TLM have been recognised since the early stage of development. Originally, only the factors describing the actual sub-cellular width of such elements have been added [1]; later, analytical [2]..[6] or empirical [7]..[9] expressions for the singular field behaviour have also been utilised. In the case of separable structures like slots in waveguide filters, a competitive approach consists in segmentation and replacing such a slot by its Z-matrix [10] or S-matirix [11] description, but this is not applicable to general 3D geometries.

Usually, the singularity corrections for metal edges or corners serve to modify field updating coefficients. Only in [6] matrix equations and coupling between the neighbouring nodes are added. Thus [6] appears to be the most rigorous method proposed so far, but at the expense of more cumbersome implementation and difficult to predict numerical properties. The purpose of this work is to evaluate whether accuracy comparable to [6] can be achieved by simpler means. It is shown that:

- Earlier methods incorporating the singular field behaviour [2]..[5] have effectively used only the radial part of analytical expressions. While these "radial models" improve the convergence over raw FDTD, they retain substantial singularity errors.
- The accuracy and convergence can be improved by an order in magnitude if we incorporate full stereoscopic expresssions for the singular fields such as shape of field lines and curvature of integration surfaces.
- The "stereoscopic models" derived herein require no additional memory or processing in comparison to "radial models". Yet for the reported benchmark they provide the same order of accuracy as the method of [6].

II. MODEL DEVELOPMENT

Let us start from the typically used Laurent series for longitudinal electric and magnetic fields in the vicinity of a metal edge [2]:

$$E_z = \Sigma\, c_k\, r^{k\nu} \sin(k\nu\,\phi) \qquad (1)$$

where the summation extends over k 1, and:

$$H_z = \Sigma\, d_k\, r^{k\nu} \cos(k\nu\,\phi) \qquad (2)$$

where the summation extends over k 0,
angle ϕ is calculated from one planar surface of metal edge to the other, and coefficient ν is given by:

$$\nu = \pi / (2\pi - \alpha) \qquad (3)$$

where α is the edge angle (e.g. α=0 in Fig.1).

Therefrom we can derive the leading term expressions for radial electric and angular magnetic fields:

$$E_r \quad e_0\, r^{\nu-1} \sin(\nu\,\phi) \qquad (4)$$

$$H_\phi \quad h_0\, r^{\nu-1} \sin(\nu\,\phi) \qquad (5)$$

An important consequence of (4)(5) is singular behaviour of the fields along the radial direction. It entails e.g. that the line integrals of radial E-fields along cell edges needed for Faraday law implementation become:

$$\int E_r\, dr = k_r E_{r0}\, \Delta r \qquad (6)$$

where $E_{r0}\Delta r$ is the result of integration assumed in raw FDTD, incorporating linear field behaviour. For example, the line integral between (x_0, y_0) and $(x_0+\Delta x, y_0)$ in Fig.1 now reads:

$$\int E_x\, dx = k_r\, E_{x0}\, \Delta x = k_r\, E_x(x_0+0.5\Delta x, y_0)\, \Delta x \qquad (7)$$

Such singularity factors k_r have also been derived by previous authors [2]..[5]. For edges aligned with the FDTD mesh and α=0 as in Fig.1, they become [3][4]:

$$k_r = \square 2 \quad 1.41 \qquad (8)$$

With reference to Fig.1 and [4], these values of k_r will also change as a function of radial edge penetration into $x>x_0$ or recession into $x<x_0$, but please note that they will remain invariant upon cells aspect ratio. They also

0-7803-7695-1/03/$17.00 © 2003 IEEE

neglect any angular and vector direction information contained in eqs.(4)(5). Thus, we shall further call them "radial models", and explore as well as correct their limitations.

For clarity, let us focus on TE polarisation in Fig.1. The raw FDTD updates the E_{x0} value needed in (7) over a time step Δt through:

$$\Delta E_{x0}/\Delta t = (H_2 - H_1)/\Delta y \qquad (9)$$

This is equivalent to saying that the surface taken for E-flux integration in Ampere law is a flat rectangle stretched between the $(x_0+0.5\Delta x,\ y_0-0.5\Delta y)$ and $(x_0+0.5\Delta x,\ y_0+0.5\Delta y)$ nodes, and that E_{x0} comes as an average of the so integrated field. However, this is in contradiction to eq.(4) since the dominant E-field close to the edge is radial and therefore:

- The surface of integration should be an arc connecting $(x_0+0.5\Delta x,\ y_0-0.5\Delta y)$ and $(x_0+0.5\Delta x,\ y_0+0.5\Delta y)$, as shown in Fig.1b, of radius r such that: $r^2 = 0.5(\Delta x^2+\Delta y^2)$, and length $l = r\,\Delta\phi$.
- The value of ΔE_{x0} obtained after replacing Δy with l in (10) does not correspond to the mid-edge value, but to the value at $x=x_0+r$.

Taking advantage of the above two observations, we can extend the one-dimensional radial singularity coefficients k_r towards multidimensional (or stereoscopic) coefficients, $k = k_r\, k_\phi$, which for the case of Fig.1 become:

$$k = \frac{\sqrt{2}}{\frac{\Delta x}{\Delta y}\arctan\frac{\Delta y}{\Delta x} + \sqrt{1+\left(\frac{\Delta y}{\Delta x}\right)^2}} \qquad (10)$$

Furthermore, at E_x node of Fig.1 we may also take into consideration angular field behaviour as $\sin(v\phi)$ in eq.(4), producing:

$$k = \frac{\sqrt{2}}{\frac{\Delta x}{\Delta y}\,2\sin\left[0.5\arctan\frac{\Delta y}{\Delta x}\right] + \sqrt{1+\left(\frac{\Delta y}{\Delta x}\right)^2}} \qquad (11)$$

By physical considerations of field line geometry (see Fig.1 right), in the half-plane $x<x_0$ eq.(4)(5) can no longer describe the dominant fields and thus eq.(11) is irrelevant for E_y nodes. For the case of Fig.1, eqs.(10) and (11) yield 1.516 and 1.57, respectively.

Let us note that singularity terms for magnetic fields are inverses of those for the orthogonal electric fields.

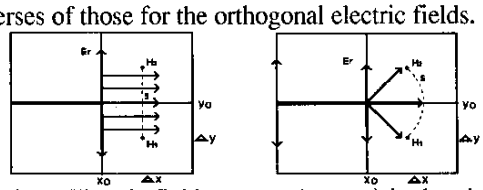

Fig.1: Electric field patterns (arrows) in the vicinity of a metal edge (along cell edge for $y=y_0$, $x<x_0$) inherent in earlier radial singularity models [3]..[5] (left) and stereoscopic models developed herein (right).

III. TEM Wave Problems

The first set of tests concerns a shielded stripline shown on the left of Fig.2. For the coarsest discretisation of a=1mm, the strip is resolved into 2 cells and the slots into 3 cells. It is important to note that the three FDTD algorithms: without any field singularity models, with radial models as in [2]..[5], and with stereoscopic models proposed herein – all use the same field updating equations and differ only in terms of sigularity factors applied to radial electric and azimuthal magnetic fields. From the numerical viewpoint, an optimum value of this factor will be that which leads to a maximally flat pattern of characteristic impedance versus discretisation. From Fig.2 we confirm that the value of k=1.516 dictated by eq.(10) excellently serves this purpose (red curve). The value of 1.41 stemming from radial models provides a substantial improvement over raw FDTD, but underestimates the strength of singularities. The simulations with k 1.53 are overweighed and produce decreasing values of impedance with refined discretisation. With k=1.516 at E_y nodes and k=1.57 after (11) at E_x node we obtain a curve indistinguishable from the red one.

Tab.1 lists numerical values of the errors associated with the curves of Fig.2. The reference value of 99.822Ω has been obtained through the very fine mesh simulation (a=0.01mm) with k=1.516.

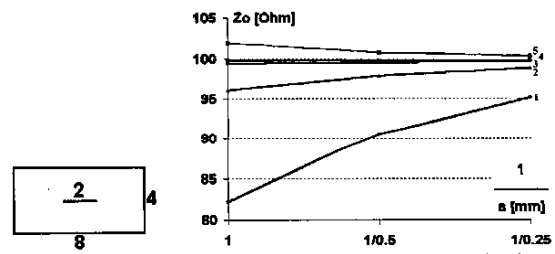

Fig.2: Characteristic impedance of shielded strip-line for various values of singularity factors; fom the lowest curve up: curve 1 – 1.00 (raw FDTD), curve 2 - 1.41 (radial), curve 3 - 1.516 (stereoscopic), curve 4 – 1.53, curve 5 – 1.6.

	raw FDTD	radial	stereoscopic
1mm	17.64	3.54	0.37
0.5 mm	9.24	1.81	0.24
0.25 mm	4.73	0.91	0.12

Tab.1: Absolute values of relative errors [%] of characteristic impedance calculation for three FDTD algorithms applied to the line of Fig.2.

A variety of tests have been run, confirming that the value of k=1.516 remains adequate for inhomogeneous (Fig.3) and asymmetrical lines (Fig.4) on equidistant meshes. Then, non-equidistant meshes have been

analysed as in Tab.2. As expected, the raw FDTD is least accurate, and interestingly its error is governed by the larger of the cell dimensions. The radial models maintain constant factor of k=1.41 after (8) and hence underestimate the contributions of E-field integrals along shorter cell sides. Their error actually increases as one of the cell dimensions is decreased. The stereoscopic models are also to some extent susceptible to this phenomenon, but retain the error at the level of 1% for aspect ratios less than 4:1.

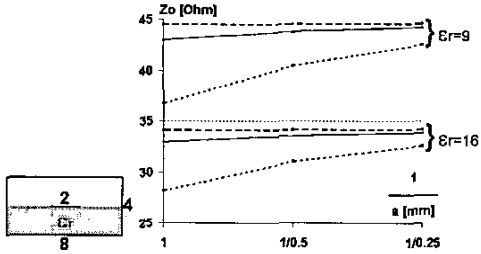

Fig.3: Characteristic impedance of inhomogeneous shielded strip line for various values of singularity factors: dotted – 1.00 (raw FDTD), continuous – 1.41 (radial model), dashed – 1.516 (our stereoscopic model).

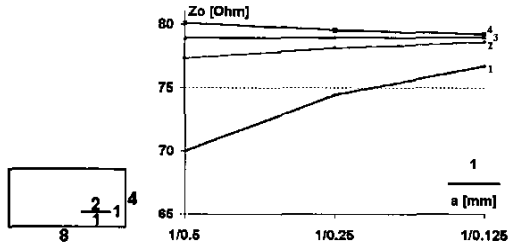

Fig.4: Characteristic impedance of shielded strip line with offset strip, for various values of singularity factors; from lowest curve up: curve 1 – 1.00 (raw FDTD), curve 2 – 1.41 (radial model), curve 3 – 1.516 (our stereoscopic model), curve 4 – 1.6.

Δy / Δx	1 mm	0.5 mm	0.25 mm
1 mm	17.64	14.45	16.49
	3.54	5.00	7.96
	0.37	0.49	1.73
0.5 mm	13.98	9.24	8.46
	4.57	1.81	2.39
	0.63	0.24	0.38
0.25 mm	12.88	7.24	4.73
	7.35	2.53	0.91
	1.81	0.16	0.12

Tab.2: Absolute values of relative errors [%] of characteristic impedance calculated by raw FDTD (top entries in each table cell), FDTD with radial singularity models (middle) and FDTD with stereoscopic singularity models (bottom) for the line of Fig.2.

IV. Examples of Cut-off Problems

Examples of Section III confirm high accuracy of the proposed stereoscopic models for TEM waves, which travel along the metal edge. Now we will consider the case of Poynting vector lying in the plane perpendicular to the edge (in xy-plane of Fig.1), as for TE and TM modes at cut-off. To ensure that we will be evaluating the effects of different field patterns and not of drastic changes in geometry approximation, we need to analyse a waveguide of cross-section resolved similarly as in our previous examples, that is, with the coarsest discretisation into approximately 10x10 cells and strips and slots extending over 2-3 cells. Such an example is a finline available in [6] and shown in Fig.5. Since the method proposed in [6] is the most advanced so far, we can consider it as a benchmark reference for the method proposed herein.

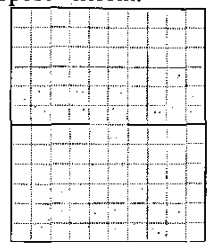

Fig.5: Geometry of finline after [6], constructed in a 5mm x 6mm waveguide, with 2mm long fins, shown here with the basic 0.5mm meshing.

Tab.3 lists cut-off frequencies of TEee1, TEoe1, and TMee1 modes obtained: in [6] for the 10x12 mesh shown in Fig.5; by raw FDTD and with our models, for successively refined mesh. The reference values are those produced by our method when converged within 0.0025 GHz, which occurs between 0.005mm and 0.025mm cell size.

	Ref.	Raw FDTD			Our models			[6]
	[GHz]	[%]			[%]			[%]
a[mm]	0.025	0.5	0.25	0.125	0.5	0.25	0.125	0.5
TE_{oe1}	15.91	-9.24	-4.46	-1.77	-0.25	-0.12	-0.03	0.06
TE_{ee1}	30.735	-1.71	-0.86	-0.42	0.05	-0.02	0.00	-0.02
TM_{ee1}	55.84	2.40	1.41	0.75	0.25	0.03	0.00	0.02

Tab.3: Cut-off frequencies [GHz] and relative errors [%] produced by raw FDTD, our stereoscopic models, and the method of [6], for specified cell-sizes.

Let us start with basic observations on the raw FDTD method. For commensurate geometry resolution the raw FDTD method induces (on average) twice smaller errors into the calculated cut-off frequencies of TE modes (Tab.3) than into characteristic impedance of TEM modes (e.g. Tab.1). This is physically justified by the fact that in TE modes at cut-off only the transverse E-field is singular, while the longitudinal H-field, by virtue of (2), is not. In the TEM wave, both transverse E- and H-fields are singular as in (4)(5). Their inaccurate approximation causes inversely proportional changes of unit inductance and unit capacitance, and hence multiplicative error of characteristic impedance.

Please also note that since raw FDTD extrudes metal edges and corners, characteristic impedance as well as cut-off frequencies of TE modes are underestimates of their physical values. To the contrary, cut-off frequencies of TM modes are loaded with positive singularity errors, compensating and even outweighing the numerical dispersion errors. This justifies an apparently good performance of raw FDTD for high-frequency poorely-resolved TM mode in Tab.3. It also explains why positive FDTD errors have been barely reported in the literature, while downward frequency shift has been considered a major concern [8].

The proposed stereoscopic singularity models (10)(11) enhance the values of radial E-fields at metal edges, and further their linear integrals in the radial direction; inversely proportionally they suppress the H-field contributions. Hence, they serve to restore the singular field behaviour on FDTD meshes. The singularity factor of 1.516 previously confirmed optimum for TEM problems also reduces the errors of cut-off frequencies extraction to 0.25% on the coarsest mesh. Although not shown in Tab.3, it has been checked that lower values of the singularity factor lead to poorer convergence for TE modes while higher values – to reversed convergence, that is, overestimating TE and underestimating TM cut-off frequencies.

V. Conclusions

New local FDTD field singularity models have been proposed. In extension to previous local models, not only radial field variation but also the geometry of field lines and curvature of Ampere / Faraday integration surfaces are taken into account. This changes the values of field updating coefficients, but requires no further modification of the basic FDTD equations. In spite of such simplicity, the accuracy obtained is of the same order as that of a specialised higher-order algorithm of [6].

As an additional outcome, this work recommends the use of characteristic impedance of TEM lines as the most sensitive testing function for any new singularity models. For comparable and reasonably coarse geometry resolution, raw FDTD produces cut-off frequencies of TM modes with 2%, TE modes with 9%, while TEM characteristic impedance with 18% errors. The stereoscopic models suppress all these errors to below 1%. The errors of previously used radial models are by order of magnitude higher than those of the new approach. Moreover, in the case of non-equidistant meshing they rapidly increase and reach half of raw FDTD errors at 4:1 aspect ratio, while under the same conditions the accuracy of stereoscopic models oscillates around 1%.

Application of stereoscopic and radial models to metal edges not aligned with the FDTD mesh lines and additional numerical stability constraints arising therefrom will be discussed in the Transactions paper.

Acknowledgement

This work has been performed within EUREKA E!2602 initiative and co-financed by the Polish State Committee for Scientific Research under grant No. 134/E-365/SPUB-M/EUREKA/T-10/DZ 206.

References

[1] A.Taflove, *Computational Electrodynamics: The Finite-Difference Time-Domain Method*, Chapter 10, Boston-London: Artech House, 1995.

[2] G.Mur, "The modelling of singularities in the finite-difference approximations of the time-domain electromagnetic-field equations", *IEEE Trans. Microwave Theory Tech.*, vol.MTT-29, No.10, Oct.1981, pp.1073-1077.

[3] J.Van Hese, D.De Zutter, "Modeling of discontinuities in general coaxial waveguide structures by the FDTD method", *IEEE Trans. Microwave Theory Tech.*, vol.MTT-40, No.3, March 1992, pp.547-556.

[4] D.B.Shorthouse, C.J.Railton, "The incorporation of static field solutions into the finite difference time domain algorithm", *IEEE Trans. Microwave Theory Tech.*, vol.MTT-40, No.5, May 1992, pp.986-994.

[5] K.Beilenhoff, W.Heinrich, "Treatment of field singularities in the finite-difference approximation", *IEEE MTT-S Int. Microwave Symp. Dig.*, 1993, pp.979-982.

[6] P.Przybyszewski, M.Mrozowski, "A conductive wedge in Yee's mesh", *IEEE Microwave & Guided Wave Lett.*, vol.8, No.2, Feb.1998, pp.66-68.

[7] W.K.Gwarek, "Analysis of arbitrarily-shaped planar circuits – a time domain approach", *IEEE Trans. Microwave Theory Tech.*, vol.MTT-33, No.10, Oct.1985, pp.1067-1072.

[8] U.Muller, P.P.M.So, W.J.R.Hoefer, "The compensation of coarseness error in 2D TLM modeling of microwave structures", *IEEE MTT-S Int. Microwave Symp. Dig.*, 1992.

[9] C.J.Railton, "An investigation into the properties of the FDTD mesh with application to wires and strips", *Int.J.Numer.Model.*, vol.12, no.1/2, pp.69-80, Jan.-April 1999.

[10] A.S.Rong, H.Yang, X.H.Chen, A.Cangellaris, "Efficient FDTD modeling of irises/slots in microwave structures and its application to the design of combline filters", *IEEE Trans. Microwave Theory Tech.*, vol.MTT-49, No.12, Dec.2002, pp.2266-2275.

[11] W.K.Gwarek, M.Celuch-Marcysiak, "A generalized approach to wide-band S-parameter extraction from FD-TD simulations applicable to evanescent modes in inhomogeneous guides", *IEEE MTT-S Int. Microwave Symp. Dig.*, 2001, pp.885-888.